

Enol Tautomers of Watson–Crick Base Pair Models Are Metastable Because of Nuclear Quantum Effects

Alejandro Pérez,[†] Mark E. Tuckerman,[‡] Harold P. Hjalmarson,[¶] and O. Anatole von Lilienfeld^{*¶}

Department of Chemistry, New York University, New York, New York 10003, Department of Chemistry and Courant Institute of Mathematical Sciences, New York University, New York, New York 10003, and Sandia National Laboratories, Albuquerque, New Mexico 87185

Received March 9, 2010; E-mail: oavonli@sandia.gov

Abstract: Intermolecular enol tautomers of Watson–Crick base pairs could emerge spontaneously via interbase double proton transfer. It has been hypothesized that their formation could be facilitated by thermal fluctuations and proton tunneling, and possibly be relevant to DNA damage. Theoretical and computational studies, assuming classical nuclei, have confirmed the dynamic stability of these rare tautomers. However, by accounting for nuclear quantum effects explicitly through Car–Parrinello path integral molecular dynamics calculations, we find the tautomeric enol form to be dynamically metastable, with lifetimes too insignificant to be implicated in DNA damage.

Introduction

In their seminal paper, Watson and Crick highlighted the importance of pyrimidine and purine bases to occur in their most plausible tautomeric form, that is, their keto- rather than their enol form, to produce correct matching.¹ A decade later, however, it was hypothesized² that proton tunneling could significantly enhance the formation of the rare tautomeric enol-forms, and thereby cause mismatch in the interstrand pairing of nucleobases, possibly leading to errors in DNA replication. These rare tautomeric enol-form could spontaneously emerge through the antiparallel and concerted transfer of two hydrogen-bonded protons between adenine (A) and thymine (T), and between cytosine (C) and guanine (G). This hypothesis rests on the assumption that rare tautomers are dynamically stable and would persist on a time scale sufficiently long as to alter the cell's genetic information via the formation of mismatches. This conjecture was further supported by several computational studies suggesting that at least the GC tautomers would have sufficient lifetime to induce DNA damage through base pair mismatches.^{3–12}

NMR studies have failed to find conclusive evidence for intermolecular tautomers of DNA bases.¹³ Experimental studies were also reported on the intermolecular tautomeric equilibrium of nucleobase pair analogues in the electronic excited state, which seem to favor rare tautomers: Kasha and co-workers detected the product tautomers in solutions of 7-azaindole dimer after photoexcitation.¹⁴ More recently, Zewail et al. followed in real time the tautomerization of the same system using femtosecond techniques.¹⁵ The product tautomer was detected and monitored using time-of-flight mass spectrometry, and these experiments provided insight into some mechanistic aspects of the decay.

Although the bonding pattern in 7-azaindole dimer (two N···H–N intermolecular hydrogen bonds) differs slightly from the canonical DNA base pairs (N–H···O and N···H–N), the authors noted the importance of quantum tunneling for this process. Using isotope substitutions in the intermolecular H-bonds, a dramatic increase in lifetime of the rare tautomer was found upon deuteration.¹⁵ Experimental studies on other tautomerizable nucleobase analogues have also been reported.^{16–19} Intramolecular proton transfer was studied spectroscopically in

[†] Department of Chemistry, New York University.

[‡] Department of Chemistry and Courant Institute of Mathematical Sciences, New York University.

[¶] Sandia National Laboratories.

(1) Watson, J. D.; Crick, F. H. C. *Nature* **1953**, *171*, 737–738.

(2) Löwdin, P. O. *Rev. Mod. Phys.* **1963**, *35*, 724–732.

(3) Florián, J.; Hroudá, V.; Hobza, P. *J. Am. Chem. Soc.* **1994**, *116*, 1457–1460, see Figure 2.

(4) Florián, J.; Leszczynski, J. *J. Am. Chem. Soc.* **1996**, *118*, 3010–3017, see Figure 2b.

(5) Podolyan, Y.; Gorb, L.; Leszczynski, J. *J. Phys. Chem. A* **2002**, *106*, 12103–12109.

(6) Gorb, L.; Podolyan, Y.; Dziekonski, P.; Sokalski, W. A.; Leszczynski, J. *J. Am. Chem. Soc.* **2004**, *126*, 10119–10129, see Table 3.

(7) Noguera, M.; Sodupe, M.; Bertran, J. *Theor. Chem. Acc.* **2004**, *112*, 318–326.

(8) Zoete, V.; Meuwly, M. *J. Chem. Phys.* **2004**, *121*, 4377–4388.

(9) Bertran, J.; Oliva, A.; Rodríguez-Santiago, L.; Sodupe, M. *J. Am. Chem. Soc.* **1998**, *120*, 8159–8167.

(10) Villani, G. *Chem. Phys.* **2005**, *316*, 1–8.

(11) Villani, G. *Chem. Phys.* **2006**, *324*, 438–446.

(12) Cerón-Carrasco, J. P.; Requena, A.; Michaux, C.; Perpéte, E. A.; Jacquemin, D. *J. Phys. Chem. A* **2009**, *113*, 7892–7898.

(13) Rüterjans, H.; Kaun, E.; Hull, W. E.; Limbach, H. H. *Nucleic Acids Res.* **1982**, *10*, 7027–7039.

(14) Taylor, C. A.; El-Bayoumi, M. A.; Kasha, M. *Proc. Natl. Acad. Sci. U.S.A.* **1969**, *103*, 253–260.

(15) Douhal, A.; Kim, S.; Zewail, A. *Nature* **1995**, *378*, 260–263.

(16) Ogawa, A. K.; Abou-Zied, O. K.; Tsui, V.; Jimenez, R.; Case, D. A.; Romesberg, F. E. *Phys. Chem. Chem. Phys.* **2000**, *122*, 9917–9920.

(17) Nishio, H.; Ono, A.; Matsuda, A.; Ueda, T. *Nucleic Acids Res.* **1992**, *20*, 777–782.

(18) Tamm, C.; Strazewski, P. *Angew. Chem., Int. Ed.* **1990**, *29*, 36–57.

(19) Singer, B.; Chavez, F.; Goodman, M. F.; Essigmann, J. M.; Dosanjh, M. K. *Proc. Natl. Acad. Sci. U.S.A.* **1989**, *86*, 8271–8274.

59 isolated nucleobase guanine^{20,21} or uracil.²² However, to date,
60 no direct experimental evidence has been reported in support
61 of the existence of the rare enol tautomers of DNA base pairs.
62 It is, therefore, an open question whether nuclear quantum
63 effects facilitate or hamper their formation.

64 The goal of this study is to investigate the role of nuclear
65 quantum effects in the double proton transfer between
66 Watson–Crick base pairs. To this end, we perform a compu-
67 tational experiment in which we simulate the double proton
68 transfer with and without nuclear quantum effects. For the
69 former, the Feynman path integral formalism was used.^{23,24}
70 Several other methods have been developed to study nuclear
71 quantum effects in the calculation of molecular properties,
72 including wave packet methods for quantum dynamics,²⁵
73 generalized transition state theory,^{26–28} dispersed polaron
74 method,²⁹ nuclear orbital and molecular orbital method,^{30,31}
75 nuclear-electron orbital method,^{32,33} non-Born–Oppenheimer
76 DFT,³⁴ and multicomponent DFT.³⁵ For our calculations, we
77 chose well-known methods to investigate our hypothesis.

78 We compare results from Car–Parrinello molecular dynamics
79 and Car–Parrinello path integral molecular dynamics (CP-
80 PIMD)^{36,37} simulations of corresponding DNA base pair models
81 at ambient temperature in the gas-phase. The CP-PIMD method
82 has been recently applied to model the nuclear quantum behavior
83 of proton transfer in hydrogen-bonded systems, both in the gas
84 phase^{38–41} and in the bulk.^{42,43} The PI, or quantized classical
85 path methods, were also shown to be relevant in biological

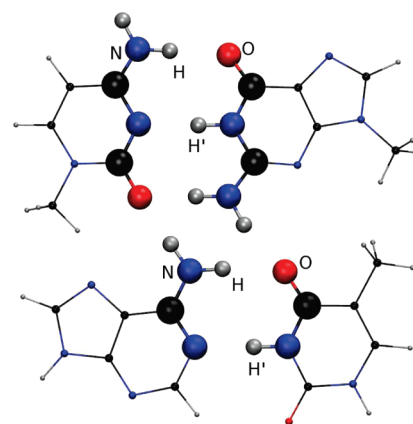


Figure 1. Canonical Watson–Crick base pairs superimposed on model systems. H' is the most acidic proton and the reaction coordinate $\xi(\mathbf{r}) = r_{\text{HN}} - r_{\text{HO}}$ for the double proton transfer involves the less acidic proton, H. (Top) GC model (guanidyl-formaldehyde–methanimidamidyl-formide, big spheres) superimposed on GC (smaller spheres). (Bottom) AT model (formamide–formamidine, big spheres) superimposed on AT (smaller spheres). To satisfy valency for the calculations, hydrogen atoms were added to both models.

86 systems such as enzymes⁴⁴ for which methods capable of
87 dealing with nuclear quantum effects have recently been
88 reviewed.⁴⁵

89 In first principles PIMD, the nuclei are quantized following
90 Feynman's path integral formalism^{23,24} and the many-body
91 potential is obtained “on-the-fly” from an electronic structure
92 calculation.^{46,47} Thus, CP-PIMD accounts not only for thermal
93 fluctuations and bond rearrangements, but also for nuclear
94 tunneling and zero point energy effects. Our findings are in
95 agreement with recent approximate quantum dynamics calcula-
96 tions by Shigeta et al. who investigated the isotope effect in
97 the double proton transfer in DNA base pairs at 0 K using a
98 two-dimensional fit of a reduced potential energy surface.⁴⁸ The
99 importance of quantizing all degrees of freedom is emphasized,
100 however. As previously reported by one of us,³⁸ not only the
101 transferring proton species, but also the heavy-atom skeleton
102 should be quantized as the latter has significant effects on proton
103 tunneling. To the best of our knowledge, a full path-integral
104 description of the double proton transfer in DNA base pair
105 models has not previously been reported.

Computational Methodology

Model Systems of DNA Bases. We have performed a set of
107 Car–Parrinello molecular dynamics calculations with classical (CP-
108 MD) and quantized nuclei (CP-PIMD) for two model systems that
109 closely mimic the hydrogen-bonding pattern of the two DNA
110 Watson–Crick base pairs. These model systems are depicted in
111 Figure 1. The AT model was previously investigated⁵ keeping the
112 F1

- (20) Nir, E.; Janzen, C.; Imhof, P.; Kleinermanns, K.; de Vries, M. S. *J. Chem. Phys.* **2001**, *115*, 4604–4611.
(21) Mons, M.; Dimicoli, I.; Piuze, F.; Tardivel, B.; Elhanine, M. *J. Phys. Chem. A* **2002**, *106*, 5088–5094.
(22) Bakker, J. M.; Sinha, R. K.; Besson, T.; Brugnara, M.; Tosi, P.; Salpin, J.-Y.; Matre, P. *J. Phys. Chem. A* **2008**, *112*, 12393–12400.
(23) Feynman, R. P. *Rev. Mod. Phys.* **1948**, *20*, 367–387.
(24) Feynman, R. P.; Hibbs, A. R. *Quantum Mechanics and Path Integrals*; McGraw-Hill: New-York, 1965.
(25) Heller, E. J. *J. Chem. Phys.* **1975**, *62*, 1544–1555.
(26) Truhlar, D. G.; Isaacson, A. D.; Garrett, B. C. Generalized Transition State Theory. In *Theory of Chemical Reaction Dynamics*; Baer, M., Ed.; CRC Press: Boca Raton, FL, 1985; Vol. 4, pp 65–137.
(27) Fernandez-Ramos, A.; Ellingson, B. A.; Garrett, B. C.; Truhlar, D. G. Variational Transition State Theory with Multidimensional Tunneling. In *Reviews in Computational Chemistry*; Lipkowitz, K. B., Cundari, T. R., Eds.; Wiley-VCH: Washington, DC, 2007; Vol. 23, pp 125–232.
(28) Meana-Paada, R.; Truhlar, D. G.; Fernandez-Ramos, A. *J. Chem. Theory Comput.* **2010**, *6*, 6–17.
(29) Warshel, A.; Hwang, J.-K. *J. Chem. Phys.* **1986**, *84*, 4938–4957.
(30) Tachikawa, M.; Mori, K.; Nakai, H.; Iguchi, K. *Chem. Phys. Lett.* **1998**, *290*, 437–442.
(31) Nakai, H. *Int. J. Quantum Chem.* **2002**, *86*, 511–517.
(32) Shigeta, Y.; Takahashi, H.; Yamanaka, S.; Mitani, M.; Nagao, H.; Yamaguchi, K. *Int. J. Quantum Chem.* **1998**, *70*, 659–669.
(33) Webb, S. P.; Iordanov, T.; Hammes-Schiffer, S. *J. Chem. Phys.* **2002**, *117*, 4106–4118.
(34) Capitani, J. F.; Nalewajski, R. F.; Parr, R. G. *J. Chem. Phys.* **1982**, *76*, 568–573.
(35) Kreibich, T.; Gross, E. K. U. *Phys. Rev. Lett.* **2001**, *86*, 2984–2987.
(36) Marx, D.; Parrinello, M. *J. Chem. Phys.* **1996**, *104*, 4077–4082.
(37) Tuckerman, M. E.; Marx, D.; Klein, M. L.; Parrinello, M. *J. Chem. Phys.* **1996**, *104*, 5579–5588.
(38) Tuckerman, M. E.; Marx, D. *Phys. Rev. Lett.* **2001**, *86*, 4946–4949.
(39) Miura, S.; Tuckerman, M. E.; Klein, M. L. *J. Chem. Phys.* **1998**, *109*, 5290–5299.
(40) Morrone, J. A.; Car, R. *Phys. Rev. Lett.* **2008**, *101*, 017801.
(41) Tuckerman, M. E.; Marx, D.; Klein, M. L.; Parrinello, M. *Science* **1997**, *275*, 817–820.
(42) Marx, D.; Tuckerman, M. E.; Hutter, J.; Parrinello, M. *Nature* **1999**, *397*, 601–604.
(43) Tuckerman, M. E.; Marx, D.; Parrinello, M. *Nature* **2002**, *417*, 925–929.

- (44) Hwang, J.-K.; Warshel, A. *J. Am. Chem. Soc.* **1996**, *118*, 11745–11751.
(45) Pu, J.; Gao, J.; Truhlar, D. G. *Chem. Rev.* **2006**, *106*, 3140–3169.
(46) Car, R.; Parrinello, M. *Phys. Rev. Lett.* **1985**, *55*, 2471–2474.
(47) Ifimie, R.; Minary, P.; Tuckerman, M. E. *Proc. Natl. Acad. Sci. U.S.A.* **2005**, *102*, 6654–6659.
(48) Shigeta, Y.; Miyachi, H.; Matsui, T.; Hirao, K. *Bull. Chem. Soc. Jpn.* **2008**, *81*, 1230–1240.
(49) Kennard, O. *J. Biomol. Struct. Dyn.* **1985**, *3*, 205–226.
(50) Kwon, O.-H.; Zewail, A. H. *Proc. Natl. Acad. Sci. U.S.A.* **2007**, *104*, 8703–8708.
(51) Kaveláč, M.; Hobza, P. *Phys. Chem. Chem. Phys.* **2007**, *9*, 903–917.
(52) Colson, A. O.; Besler, B.; Sevilla, M. D. *J. Phys. Chem.* **1992**, *96*, 9787–9794.
(53) Colson, A. O.; Besler, B.; Sevilla, M. D. *J. Phys. Chem.* **1992**, *96*, 661–668.

Table 1. Relative Energies (kcal/mol) for Structures Corresponding Approximately to Reactants (R), the Transition State (TS), and Products (P) for GC and AT Model Systems

method	GC model			AT model		
	ΔE_{P-R}	ΔE_{TS-P}	ΔE_{TS-R}	ΔE_{P-R}	ΔE_{TS-P}	ΔE_{TS-R}
RHF	13.50	14.65	28.15	11.80	9.47	21.27
MP2	9.37	4.04	13.41	8.62	4.37	12.99
CC2	10.24	2.67	12.91	9.24	3.08	12.32
PBE0	10.95	3.00	13.95	8.93	2.81	11.74
PBE	10.63	0.55	11.18	8.56	1.19	9.75
B3LYP	11.39	4.78	16.17	9.47	3.52	12.99
BLYP	11.16	3.15	14.31	9.30	2.44	11.74

nuclei classical, whereas the GC model is proposed here for the first time, and has been validated (to be discussed later) by comparing its energetics to the full GC base pair results.⁴ We assume these models to be sufficiently representative for the description of the double proton transfer of their full base pair counterparts.

The effects of the phosphate backbone, or the π - π stacked neighboring base pairs, are second-order effects as recently shown by Zoete and Meuwly,⁸ and are unlikely to affect qualitatively our findings. These authors found similar reaction barriers for the double proton transfer in isolated GC pair as well as the GC pair embedded in DNA strand (see Figure 3 in ref 8). The consideration of all these secondary effects is prohibitive in the path integral setting and our aim here is to quantify the contribution of nuclear quantum effects to the double proton transfer within nucleobase pairs.

Choice of the DFT Exchange-Correlation Functional. We have investigated the performance of several DFT functionals by comparing to second-order approximate coupled cluster theory (CC2) on various geometries on the potential energy surface. The comparison is displayed in Table 1 which also includes the values of other single Slater determinant methods, such as Hartree–Fock and second-order Møller–Plesset perturbation theory. All values were computed using the code TURBOMOLE⁵⁴ and the basis set *def-TZVPP*.

Table 1 shows that Hartree–Fock performs poorly and grossly overestimates all the barriers. Inclusion of electronic correlation is expected to improve the energetics. Indeed, hybrid functionals PBE0⁵⁵ and B3LYP⁵⁶ perform very well but their associated computational cost for plane wave basis set MD calculations is prohibitive. As one would expect for a generalized gradient approximated functional, PBE⁵⁷ seems to slightly underestimate barriers. Albeit known to also underestimate barriers,⁵⁸ for this process, BLYP deviates from coupled cluster at most by 1.5 kcal/mol and therefore appears to represent an acceptable compromise between accuracy and computational cost. Our BLYP values also agree well with earlier quantum chemical estimates of the full base pairs in gas phase computed at the MP2/6-31G**^{4,6} and B3LYP/6-311++G**^{7,59} level. We also confirmed the TURBOMOLE BLYP values in Table 1 with the ones obtained from our CP-MD setup (not shown).

In summary, the BLYP functional represents the best compromise between accuracy and cost for our model systems, and it is the functional adopted in our Car–Parrinello MD calculations. We note, however, that the point of this study is not to confirm BLYP's

suitability for energy barriers but rather to demonstrate the importance of nuclear quantum effects on free energy barriers at a given level of theory.

Car–Parrinello Path Integral Molecular Dynamics. All molecular dynamics simulations were performed at 300 K using the empirical generalized gradient approximation BLYP^{60–62} within the Kohn–Sham (KS) density functional theory (DFT).⁶³ All calculations were carried out at the Γ -point under isolated molecule boundary conditions as implemented by Martyna and Tuckerman⁶⁴ in CPMD.⁶⁵ The fictitious mass employed to propagate the electronic orbitals was set to 400 au. Normal mode variables were used for the discrete path integral, together with massive Nosé–Hoover chain thermostats⁶⁶ to ensure adequate canonical sampling.^{36,37} A Trotter number of 16 beads was used for the quantization of all nuclei.

For the AT model complex, valence electronic orbitals were expanded using a plane wave kinetic energy cutoff of 100 Ry in an isolated box of $12.5 \times 10.5 \times 6.5 \text{ \AA}^3$. Core electronic orbitals were represented by Goedecker pseudopotentials⁶⁷ as published by Krack.⁶⁸ For the GC model system, a plane wave cutoff of 75 Ry was used in an isolated box of $15 \times 15 \times 8 \text{ \AA}^3$. Core electronic orbitals were represented by Troullier–Martins pseudopotentials.⁶⁹

Free-Energy Sampling of Rare Events. We compute the classical potential of mean force,

$$F(\xi^*) = -\frac{1}{\beta} \ln \left[\frac{C}{Q(\beta)} \int d\mathbf{r} e^{-\beta U(\mathbf{r})} \delta(\xi(\mathbf{r}) - \xi^*) \right] \quad (1)$$

for the classical free-energy profiles along the proton transfer reaction coordinate, $\xi = \xi(\mathbf{r})$. In this expression, $Q(\beta)$ is the classical canonical configuration partition function, $C = h^{-3N}/N!$, and $U(\mathbf{r})$ is the KS-BLYP potential energy of the system at the microstate \mathbf{r} .

Direct sampling of eq 1 for rare events is difficult in ordinary MD and special techniques are required to enhance the exploration of inaccessible regions. Since the double proton transfer in AT and GC has barriers well above the thermal energy, we have combined umbrella sampling⁷⁰ with CP-PIMD and standard CP-MD to compute the free-energy profiles with and without nuclear quantum effects, respectively. Within umbrella sampling, one restrains the position of a selected reaction coordinate ξ to a certain window i (defined by a reference value ξ_i) typically using an harmonic bias

(60) Becke, A. D. *Phys. Rev. A* **1988**, *38*, 3098–3100.

(61) Colle, R.; Salvetti, D. *Theor. Chim. Acta* **1988**, *37*, 329–334.

(62) Lee, C.; Yang, W.; Parr, R. G. *Phys. Rev. B* **1988**, *37*, 785–789.

(63) Kohn, W.; Sham, L. J. *Phys. Rev.* **1965**, *140*, A1133–A1138.

(64) Martyna, G. J.; Tuckerman, M. E. *J. Chem. Phys.* **1999**, *110*, 2810–2821.

(65) CPMD version 3.13.2 Home page. Copyright IBM Corp 1990–2008, Copyright MPI für Festkörperforschung Stuttgart, 1997–2001, <http://www.cpmid.org/>.

(66) Martyna, G. J.; Klein, M. L.; Tuckerman, M. E. *J. Chem. Phys.* **1992**, *97*, 2635–2643.

(67) Goedecker, S.; Teter, M.; Hutter, J. *Phys. Rev. B* **1996**, *54*, 1703–1710.

(68) Krack, M. *Theor. Chem. Acc.* **2005**, *114*, 145–152.

(69) Troullier, N.; Martins, J. L. *Phys. Rev. B* **1991**, *43*, 1993–2006.

(70) Torrie, G. M.; Valleau, J. P. *Chem. Phys. Lett.* **1974**, *28*, 578–581.

194 potential, $U_i(\xi) = (K/2)(\xi - \xi_i)^2$. The harmonic force constant K
 195 was set to 0.1 au. A total of 14 and 11 umbrella windows were
 196 collected for AT and GC models, respectively. The length of each
 197 umbrella window was 3.6 ps and the time step was 0.072 fs. The
 198 free-energy profile is thereafter reconstructed from the biased (or
 199 non-Boltzmann) MD simulations using the weighted histogram
 200 analysis method.^{71,72}

201 In PIMD simulations, the umbrella potential is applied on the
 202 centroid mode of the ring polymer, defined by $\xi = (1/P)\sum_{s=1}^P \xi_s$,
 203 where ξ_s correspond to the reaction coordinate values of the different
 204 imaginary time slices of the ring polymer, and P is the Trotter
 205 number^{24,73} ($P = 16$ for this study). The quantum potential of mean
 206 force is computed according to eq 1 where the potential energy
 207 $U(\mathbf{r})$ and the classical partition function Q are substituted by their
 208 quantum analogues, the effective classical potential and the quantum
 209 partition function, respectively.²⁴ These forces bias the sampling
 210 of the centroids so the generalized reaction coordinate ξ remains
 211 near the reference value ξ_i defined in umbrella window i .

212 The choice of a single reaction coordinate is a nontrivial task
 213 for double proton transfer events and in principle a complete
 214 characterization of this process would require a prohibitive full two-
 215 dimensional map. Here, the relative distance involving N, O, and
 216 the less acidic proton H ($\xi(\mathbf{r}) = r_{\text{HN}} - r_{\text{HO}}$, see Figure 1) was chosen
 217 as a reaction coordinate for the GC and AT models. This reaction
 218 coordinate was used to drive the proton transfer reaction from the
 219 nitrogen of one moiety to the oxygen of the other,



220 According to previous work,⁵ for the case of the AT model, the
 221 complete proton transfer of H from N to O (see Figure 1) marks
 222 the appearance of products. By the time H migrates to O, the other
 223 proton (H') has been already transferred to preserve electroneutrality.
 224 Thus, this one-dimensional coordinate appears sufficient as it
 225 approximates well the rate-determining step of the reaction. Similar
 226 arguments hold for the GC model dimer. We note in passing that
 227 in contrast to the neutral system, single proton transfer is the favored
 228 mechanism in charged DNA bases (which may be generated by
 229 radiation or by oxidizing agents) and have been investigated
 230 computationally by Bertran and co-workers.⁹

231 Results

F2 232 **Free-Energy Profiles.** Figure 2 (top) displays the classical and
 233 the quantum free energy profile for the intermolecular double
 234 proton transfer in the GC model at 300 K. The profiles feature
 235 a prominent asymmetric barrier characteristic of a late transition
 236 state. The geometry of the product and transition state are very
 237 similar, in agreement with the Hammond postulate.⁷⁴ Classically,
 238 an equilibrium free-energy difference and a reverse barrier of
 239 approximately 10 and 4 kcal/mol, respectively, are predicted.
 240 The agreement with the literature results^{4,6,7,11,59} for classical
 241 nuclei suggests that our model system captures well the
 242 fundamental features of the double proton transfer of the
 243 complete DNA base pair system despite its lack of aromatic
 244 cores. Upon quantization of the nuclei, the reaction free energy
 245 increases approximately by 1 kcal/mol due to zero point motion
 246 with respect to the classical case. More interestingly, the reverse
 247 barrier becomes negligible (less than 1 kcal/mol), and the
 248 quantum system shows no clear minimum structure on the rare
 249 tautomer side. According to transition state theory, such a
 250 decrease in the barrier would speed up the reverse reaction by

(71) Ferrendberg, A. M.; Swendsen, R. H. *Phys. Rev. Lett.* **1988**, *61*, 2635–2638.

(72) Ferrendberg, A. M.; Swendsen, R. H. *Phys. Rev. Lett.* **1989**, *63*, 1195–1198.

(73) Chandler, D.; Wolynes, P. G. *J. Chem. Phys.* **1981**, *74*, 4078–4095.

(74) Hammond, G. S. *J. Am. Chem. Soc.* **1955**, *77*, 334–338.

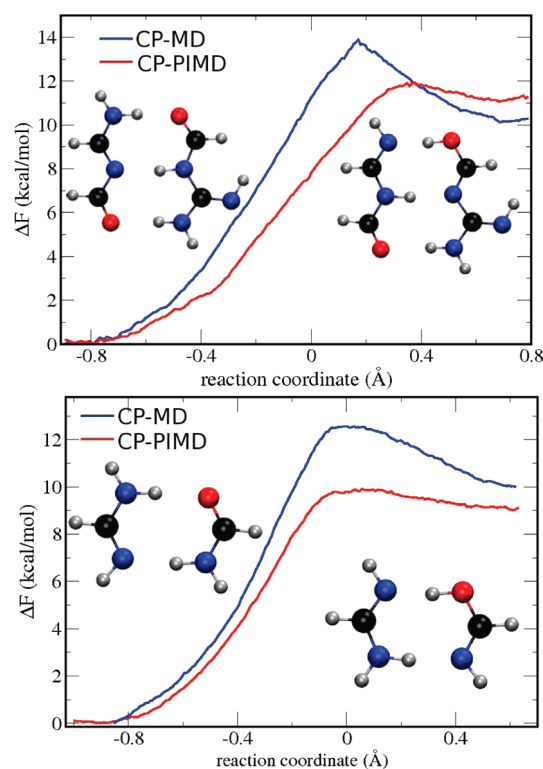


Figure 2. Classical (blue) and quantum (red) free-energy profiles for the double proton transfer in GC (top) and AT (bottom) models at 300 K. The insets show the reactants (left) and the rare tautomer products (right).

at least 2 orders of magnitude. A path integral formulation of quantum transition state theory can be found in previous work.^{75–77}

In the case of the AT model, the double proton transfer takes place via a concerted and asynchronous mechanism.⁵ Figure 2 (bottom) shows the free-energy profile for the isolated AT model at 300 K. This profile is similar to the one for the GC model dimer, although the shape of the classical barrier is smoother. Classical simulations predict a free-energy difference of approximately 10 kcal/mol between two well-defined minima, and a reverse barrier of approximately 2.5 kcal/mol. The classical free-energy barrier at 300 K agrees well with the potential energy barrier computed at 0 K (see Table 1). Also for this base pair model, nuclear quantum effects have a dramatic impact on the reverse barrier in AT model, which is reduced to less than 1 kcal/mol. In contrast to the GC base pair model, the free-energy difference between stable tautomers decreases by ~ 1 kcal/mol.

In both models, the inclusion of nuclear quantum effects decreases the forward barrier significantly, indicating that the rare tautomers are more frequently visited than within the classical picture, in accord with the original tautomeric hypothesis.² However, the virtually complete suppression of the reverse barrier, in the competing reaction, suggests that the rare tautomers are dynamically metastable and exhibit insignificant lifetimes. This prediction is in agreement with the recent work of Shigeta et al. who investigated the isotope effect in DNA base pairs using a two-dimensional fit to a reduced potential energy surface.⁴⁸

(75) Voth, G. A. *J. Phys. Chem.* **1993**, *97*, 8365–8311.

(76) Voth, G. A. *Adv. Chem. Phys.* **1996**, *93*, 135–218.

(77) Gillan, M. J. *Phys. Rev. Lett.* **1987**, *58*, 563–566.

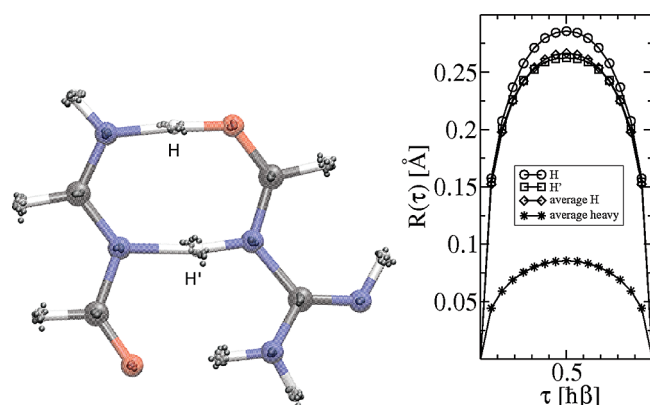


Figure 3. (Left) Snapshot of the transition state of the double proton transfer in the GC model from a typical PIMD run as presented in ref 78. H is the restrained and less acidic proton. (Right) Root mean square displacement correlation function $R(\tau)$ as a function of the normalized imaginary time, $\tau = (s - 1)/P$ (in units of $\beta\hbar$ and for $s = 1, \dots, P + 1$) for the transition state window of the double proton transfer in the GC model.

280 **Nuclear Quantum Nature.** To better illustrate the quantum
 281 delocalization of the nuclei, a snapshot⁷⁸ from typical PIMD
 282 runs at the transition state umbrella window is shown in Figure
 283 3 (top) for the GC model. The beads correspond to the
 284 discretized path in imaginary time, and their spread is evident
 285 for the light hydrogen atoms. To quantify the quantum delocalization
 286 of different nuclei, root-mean-square displacement
 287 correlation functions, $R(\tau) = \langle |\mathbf{r}_1 - \mathbf{r}_\tau|^2 \rangle^{1/2}$ (angular brackets
 288 denote canonical average) are displayed in Figure 3 (bottom)
 289 as a function of the normalized imaginary time τ . Here, $\tau = (s - 1)/P$
 290 is given in units of $\beta\hbar$, and $s = 1, \dots, P + 1$. The quantity
 291 $R(\tau = 0.5)$ is largest for the restrained proton (H) and reaches
 292 up to 0.286 Å. The quantities $R(\tau)$ for all other protons, hardly
 293 distinguishable, have been averaged, and the averaged value
 294 reaches ~ 0.02 Å less than H. Interestingly, the quantum nature
 295 of the other proton involved in the transfer (H') is slightly
 296 smaller than for the average of all other protons. As one would
 297 expect, the maximum average value of $R(\tau)$ for all heavier
 298 atoms, exhibiting less quantum nature, is significantly smaller,
 299 and reaches only 0.086 Å. For the AT model, entirely analogous
 300 behavior is found (not shown).

301 Discussion

302 On the basis of our findings it seems unlikely that the rare
 303 tautomer exists sufficiently long to contribute in any significant
 304 amount to base pair mismatch during DNA replication or
 305 translation. For externally generated (e.g., through radiation or
 306 oxidative damage) charged or radical DNA base pairs, recent
 307 computational studies^{7,9,59} using classical nuclei have shown
 308 that charged protonated base pairs display smaller activation
 309 barriers. As mentioned in the Introduction, the electronic
 310 structure in the excited state also appears to stabilize rare
 311 tautomers.¹⁵ CIS calculations in the low-energy excited single
 312 electronic state by Moreno and co-workers⁷⁹ have shown that
 313 the double proton transfer in the AT pair becomes more facile
 314 than in the ground state. Whether nuclear quantum effects have
 315 similar effects in the case of externally generated (e.g., through

radiation or oxidative damage) electronically excited, charged, 316
 or radical DNA base pairs will be a subject of future studies. 317

The models employed here have a rather small entropic 318
 contribution to the barrier in gas phase owing to the small 319
 molecular reorganization, that is, thermal fluctuations are small 320
 in a rigid heavy-atom-skeleton, playing a minor role in the 321
 proton hopping mechanism. In solution, this may not be 322
 the case, and solvent molecules may reorganize to stabilize the 323
 transition state, leading to a reduction in entropy. However, one 324
 would expect a competing effect of favorable enthalpic interac- 325
 tions with the solvent. The degree to which our results would 326
 change if the full base pairs, hydration effects,¹² coordination 327
 to a metal cation,⁶ or molecular environment were included 328
 remains to be elucidated. This effect has recently been shown 329
 to be small for classical nuclei.⁸ 330

Solvent can affect the tautomeric equilibrium between DNA 331
 bases due to the different H-bonding patterns and dipole 332
 moments of the tautomers. X-ray studies on oligonucleotides 333
 with mismatches have suggested that water could have a stabilizing 334
 effect on the nucleobase mismatch via the formation of favorable 335
 interactions with hydrophilic regions of the nucleobases.⁴⁹ In a 336
 recent study, Zewail and Kwon reexamined 7-azaindole in 337
 solution and found the rate of proton transfer is found to be 338
 significantly dependent on polarity and on the isotopic composi- 339
 tion in the pair.⁵⁰ The presence of solvent could also induce 340
 the formation of tautomers between water and a single nucleo- 341
 base, which would be relevant in the replication mechanism 342
 when DNA is unwound by the enzyme helicase. The solvent 343
 effect on the various tautomeric equilibrium of isolated DNA 344
 bases was investigated by Hobza and Kabeláč⁵¹ who studied 345
 computationally microhydrated complexes of DNA bases. 346
 Although the inclusion of solvent is currently computationally 347
 prohibitive in PIMD calculations, we remark, however, that the 348
 environment of nucleobases in DNA is different than that in 349
 free solution. The interbase hydrogen bonds are embedded in 350
 the DNA groove, protected from solvent molecules, and the 351
 DNA interior has a low dielectric constant.^{52,53} Furthermore, 352
 the attack of a water molecule on the reaction site is impeded 353
 owing to the high directionality of the hydrogen bonds. 354

Finally, another pathway that would further reduce the 355
 lifetime of unusual tautomers would be through a nonradiative 356
 decay into heat (e.g., via collision deactivation). However, our 357
 model systems, due to their isolated nature, lack the necessary 358
 coupling to other degrees of freedom for this conversion. 359
 Investigation of a more complex system is currently prohibitive 360
 within the CP-PIMD methodology. 361

362 Conclusion

CP-PIMD and standard CP-MD calculations have been 363
 carried out to study the double proton transfer reaction in isolated 364
 model systems of DNA Watson–Crick base pairs AT and GC 365
 at 300 K. Our results suggest that nuclear quantum effects 366
 including tunneling and zero point motion play a decisive role. 367
 Their inclusion leads to a near complete suppression of the 368
 reverse barrier from the rare enol to the canonical keto tautomer, 369
 thereby rendering the former dynamically metastable. This 370
 finding is in agreement with a recent approximate quantum 371
 dynamics calculation using a two-dimensional fit of a reduced 372
 potential energy surface.⁴⁸ At the transition state, the restrained 373
 proton is found to exhibit a larger root-mean-square displace- 374
 ment correlation function than all other protons, underscoring 375
 its delocalized quantum nature. On the basis of energetic 376
 arguments, our results are expected to carry over to the true 377

(78) For a path integral animation of the double proton transfer reaction in AT and GC models, see Supporting Information. The movies do not show any real time dynamics but only the sampling of different microstates of the system at 300 K.

(79) Guallar, V.; Douhal, A.; Moreno, M.; Lluch, J. M. *J. Phys. Chem. A* **1999**, *103*, 6251–6256.

378 Watson–Crick base pairs, unless external factors help to
379 selectively stabilize the enol rare tautomers. In this regard, it
380 will be important to examine the role of the DNA polymer and
381 the solvent. Thus, nuclear quantum effects appear to enhance
382 the dynamic stability of the canonical DNA base pair model
383 keto tautomers, rather than to facilitate the formation of the
384 tautomeric enol forms. This interpretation is consistent with the
385 aforementioned lack of experimental evidence for the rare
386 intermolecular tautomers.

387 In a broader context, we support the general observation⁴⁵
388 that even at room temperature nuclear quantum effects can
389 qualitatively affect the expected outcome of processes that
390 involve hydrogen-bonding, a ubiquitous feature of many
391 biological systems, such as DNA or the active sites of enzymes.

392 **Acknowledgment.** The authors thank A. E. Mattsson and P. A.
393 Schultz for many discussions. A.P. is grateful for support from

SNL's summer student internship program at the Computer Science 394
Research Institute. A.P. and H.P.H. acknowledge support from 395
SNL's LDRD project, No. 117866. M.E.T. acknowledges support 396
from NSF CHE-0704036. O.A.v.L. acknowledges support from 397
SNL's LDRD Truman program, No. 120209. Sandia is a multi- 398
program laboratory operated by Sandia Corporation, a Lockheed 399
Martin Company, for the United States Department of Energy's 400
National Nuclear Security Administration under contract DE-AC04- 401
94AL85000. 402

Supporting Information Available: Structures used in Table 403
1 and path integral animations of our DNA base pair models. 404
This material is available free of charge via the Internet at [http://](http://pubs.acs.org) 405
pubs.acs.org. 406

JA102004B 407